Am J Physiol Heart Circ Physiol 288: H2931–H2939, 2005.
First published January 11, 2005; doi:10.1152/ajpheart.01220.2004.

K^+ currents regulate the resting membrane potential, proliferation, and contractile responses in ventricular fibroblasts and myofibroblasts

L. Chilton,[1] S. Ohya,[2] D. Freed,[3] E. George,[1] V. Drobic,[3] Y. Shibukawa,[1] K. A. MacCannell,[1] Y. Imaizumi,[2] R. B. Clark,[1] I. M. C. Dixon,[3] and W. R. Giles[4]

[1]*Department of Physiology and Biophysics, University of Calgary, Calgary, Alberta, Canada;* [2]*Department of Molecular and Cellular Pharmacology, Nagoya City University, Nagoya, Japan;* [3]*St. Boniface Heart Institute, University of Manitoba, Winnipeg, Manitoba, Canada; and* [4]*Department of Bioengineering, University of California-San Diego, La Jolla, California*

Submitted 3 December 2004; accepted in final form 10 January 2005

Chilton, L., S. Ohya, D. Freed, E. George, V. Drobic, Y. Shibukawa, K. A. MacCannell, Y. Imaizumi, R. B. Clark, I. M. C. Dixon, and W. R. Giles. K^+ currents regulate the resting membrane potential, proliferation, and contractile responses in ventricular fibroblasts and myofibroblasts. *Am J Physiol Heart Circ Physiol* 288: H2931–H2939, 2005. First published January 11, 2005; doi:10.1152/ajpheart.01220.2004.—Despite the important roles played by ventricular fibroblasts and myofibroblasts in the formation and maintenance of the extracellular matrix, neither the ionic basis for membrane potential nor the effect of modulating membrane potential on function has been analyzed in detail. In this study, whole cell patch-clamp experiments were done using ventricular fibroblasts and myofibroblasts. Time- and voltage-dependent outward K^+ currents were recorded at depolarized potentials, and an inwardly rectifying K^+ (Kir) current was recorded near the resting membrane potential (RMP) and at more hyperpolarized potentials. The apparent reversal potential of Kir currents shifted to more positive potentials as the external K^+ concentration ($[K^+]_o$) was raised, and this Kir current was blocked by 100–300 μM Ba^{2+}. RT-PCR measurements showed that mRNA for Kir2.1 was expressed. Accordingly, we conclude that Kir current is a primary determinant of RMP in both fibroblasts and myofibroblasts. Changes in $[K^+]_o$ influenced fibroblast membrane potential as well as proliferation and contractile functions. Recordings made with a voltage-sensitive dye, $DiBAC_3(4)$, showed that 1.5 mM $[K^+]_o$ resulted in a hyperpolarization, whereas 20 mM $[K^+]_o$ produced a depolarization. Low $[K^+]_o$ (1.5 mM) enhanced myofibroblast number relative to control (5.4 mM $[K^+]_o$). In contrast, 20 mM $[K^+]_o$ resulted in a significant reduction in myofibroblast number. In separate assays, 20 mM $[K^+]_o$ significantly enhanced contraction of collagen I gels seeded with myofibroblasts compared with control mechanical activity in 5.4 mM $[K^+]_o$. In combination, these results show that ventricular fibroblasts and myofibroblasts express a variety of K^+ channel α-subunits and demonstrate that Kir current can modulate RMP and alter essential physiological functions.

rat ventricle; voltage clamp

CARDIAC MYOCYTES comprise ~75% of the volume of mammalian ventricles, but they account for only ~30% of all myocardial cells (50). Ninety percent of the remaining myocardial cells are cardiac fibroblasts (5). Under physiological conditions, cardiac fibroblasts are responsible for maintaining the extracellular matrix (5) and also produce a wide variety of autocrine and paracrine factors (11).

In response to ischemia and/or myocyte injury, a localized immune response is initiated. This results in fibroblast recruitment (14), and fibroblasts proliferate and transform into myofibroblasts (46). Like fibroblasts, myofibroblasts are also proliferative and mobile, and they synthesize numerous autocrine and/or paracrine factors (43). In addition, myofibroblasts can contract, and this may assist in reduction of myocardial scar size during wound resolution (44).

Despite the important roles played by cardiac fibroblasts and myofibroblasts, the ionic basis for their membrane potential is not fully understood. Furthermore, no information is available concerning whether modulation of the membrane potential of adult cardiac fibroblasts or myofibroblasts can influence their physiological function(s). Rook et al. (37) studied some of the electrophysiological characteristics of cultured neonatal rat cardiac fibroblasts. These fibroblasts were not electrically excitable, had resting membrane potentials (RMPs) between −20 and −30 mV, and expressed outwardly rectifying ionic current(s). The RMP in adult rat atrial cardiac fibroblasts is also relatively depolarized (−37 ± 3 mV) (22). In these in situ experiments, membrane potential hyperpolarized during atrial relaxation and depolarized during atrial contraction (20, 21, 23, 27–29). These oscillations in membrane potential, termed "mechanically induced potentials," were blocked by 40 μM gadolinium. Patch-clamp analysis of freshly dissociated adult rat atrial fibroblasts provided evidence for a gadolinium-sensitive nonselective cation conductance that was enhanced by compression and inhibited by stretch (22). In these freshly dissociated adult atrial fibroblasts, no conventional voltage-gated currents were identified.

In the present study, both freshly dissociated fibroblasts and cultured myofibroblasts were studied using the whole cell patch-clamp technique. The primary goal was to identify the main ionic currents and determine their role in control of RMP. After it was demonstrated that both cell populations consistently expressed K^+ currents, expression of mRNA encoding α-subunits of a variety of K^+ channels was assessed. In the final set of experiments, myofibroblasts were studied to determine whether modulation of membrane potential could affect physiological function, as judged by *1*) changes in cell number and *2*) changes in the extent of deformation of collagen I gels that had been seeded with myofibroblasts. Some of these findings have been reported recently in abstract form (8, 9). The delayed rectifier K^+ currents have been studied in detail in a recent study from our laboratory (42).

Address for reprint requests and other correspondence: W. R. Giles, Dept. of Bioengineering, Univ. of California-San Diego, 9500 Gilman Dr., La Jolla, CA 92093-0412 (E-mail: wgiles@bioeng.ucsd.edu).

The costs of publication of this article were defrayed in part by the payment of page charges. The article must therefore be hereby marked "*advertisement*" in accordance with 18 U.S.C. Section 1734 solely to indicate this fact.

MATERIALS AND METHODS

Materials. Collagenase type II was purchased from Worthington Biochemical; DMEM/F12, standard minimal essential medium, FCS, trypsin EDTA solution, fungizone, gentamycin, penicillin-streptomycin solution were purchased from GIBCO/Invitrogen; and $DiBAC_4(3)$ and collagen I were purchased from Molecular Probes and StemCell, respectively. All other chemicals were obtained from Sigma-Aldrich.

Fibroblast isolation. All procedures complied with Canadian Council on Animal Care regulations. The methods used are in compliance with the National Institutes of Health *Guide for the Care and Use of Laboratory Animals* (NIH Pub. No. 85-23, Revised 1996) and with University of Calgary guidelines. Adult male Sprague-Dawley rats were anaesthetized with isoflourane and methoxyflourane. Hearts were Langendorff perfused at 8 ml/min (37°C) with *1*) 1 mM $CaCl_2$-Tyrode solution for 5 min; *2*) $CaCl_2$-free Tyrode solution for 5 min, and *3*) 4 μM $CaCl_2$-Tyrode solution containing 0.04 mg/ml collagenase II and 0.004 mg/ml protease XIV for 9–12 min. Ventricular tissue was then cut into ~1-mm^2 pieces and further digested in 10 μM $CaCl_2$, 1 mg/ml collagenase II, 0.1 mg/ml protease XIV, and 0.5% BSA-Tyrode solution in a 37°C shaker bath.

For electrophysiological studies, fibroblasts were diluted in Krafte-Brühe buffer [containing (in mM) 100 K-glutamate, 10 K-aspartate, 25 KCl, 10 KH_2PO_4, 2 $MgSO_4$, 20 taurine, 5 creatine, 0.5 EGTA, 20 glucose, and 5 HEPES, with 1% BSA]. Cells were maintained in this medium for 1 h at 22 ± 1°C before being stored at 4°C and were used within 6 h of being refrigerated. Refrigerated cells were allowed to warm 30 min before the initiation of electrophysiological studies.

When placed under cell culture conditions, cardiac fibroblasts quickly transform into myofibroblasts (15, 47–48). To obtain a predominantly myofibroblast population, ventricular fibroblasts in KB buffer were spun (2,000 rpm, 10 min) and then resuspended in DMEM with 10% FCS, penicillin-streptomycin (10 μ/ml), gentamycin (50 μg/ml), and fungizone (0.0125 μg/ml). Cells were incubated in a 250-ml Falcon flask (VWR) in a 37°C CO_2 water-jacketed incubator (Forma Scientific). After the first passage, the majority of these cells demonstrated robust staining for smooth muscle α-actin, a marker of myofibroblasts that is absent in fibroblasts (46) (data not shown).

Electrophysiological measurements. Cells were placed on the stage of a Nikon Diaphot inverted microscope and superfused continuously at 22 ± 1°C with Tyrode solution containing (in mM) 140 NaCl, 5.4 KCl, 1 $CaCl_2$, 1 $MgCl_2$, 10 HEPES, 5.5 glucose, and 7.14 mannitol (pH adjusted to 7.4 with NaOH). Tyrode solutions with selected external K^+ concentrations ($[K^+]_o$) were prepared by isotonic substitution with NaCl. Patch pipettes were made from borosilicate glass shanks (World Precision Instruments) with a P-87 Flaming/Browning pipette puller (Sutter Instruments). Pipette tips were polished (Narishige Scientific Instrument Lab microfoge). These patch pipettes had resistances of 6–12 MΩ when filled with a solution containing (in mM) 12 NaCl, 20 KCl, 110 K-aspartate, 1 $CaCl_2$, 1 $MgCl_2$, 4 K_2ATP, 10 EGTA, and 10 HEPES (pH adjusted to 7.2 with KOH).

Whole cell voltage-clamp experiments were done using an EPC 7 amplifier (List Electronic) interfaced to a Digidata 1322A data-acquisition system controlled by Clampex version 8.1 software (Axon Instruments). Data was analyzed with pCLAMP software (Axon Instruments) and Origin 6.1 (OriginLab) and plotted as isochronal current-voltage (*I-V*) curves.

Cell capacitance was measured by integrating the capacitative transient evoked during 10-mV depolarizing steps from a holding potential of −50 mV. Input resistance was calculated from current changes in response to 10-mV depolarizing steps from a holding potential of −60 mV.

Whole cell *I-V* relationships were determined from a holding potential of −50 mV. The protocol consisted either of 500-ms voltage steps, applied in 10-mV increments between −140 mV and 30 mV, or of a 1-s voltage ramp from either −140 to 50 mV or −125 to 20 mV. Responses to $BaCl_2$ or to changing $[K^+]_o$ were obtained after their application with a rapid perfusion system (ALA Scientific Instruments). Leakage current through the pipette/plasmalemma seal was estimated from the seal resistance and applied voltages and was subtracted from raw current records. Membrane voltages have been corrected for a junction potential of 10 mV, as calculated by pCLAMP software.

Qualitative and quantitative PCR. Total RNA was extracted from P1 myofibroblasts and reverse transcribed as reported previously. The PCR amplication protocol was as follows: 15 s at 95°C and 60 s at 60°C for 1 min according to AmpliTaq Gold (Applied Biosystems; Foster City, CA). GAPDH primers were used to confirm that the products generated were representative of RNA. Each amplified product was sequenced by the chain termination method with an ABI PRIZM 3100 genetic analyzer (Applied Biosystems). Real-time quantitative PCR was performed with the use of Syber green chemistry on an ABI 7000 sequence detector (Applied Biosystems). Experimental quantities were calculated relative to the standard curve for a particular set of primers, yielding transcriptional quantitation of gene products relative to the endogenous standard (GAPDH). The reproducibility of the assay was tested by ANOVA comparing repeat runs of samples, and mean values generated at individual time points were compared by Student's *t*-test.

The following PCR primers were used: Kv1.1 (GenBank accession no. NM_173095, 357–485), amplicon = 129 bp; Kv1.2 (GenBank accession no. NM_012970, 1285–1385), amplicon = 101 bp; Kv1.5 (GenBank accession no. NM_012972, 1385–1491), amplicon = 107 bp; Kv1.6 (GenBank accession no. AJ276137, 155–259), amplicon = 105 bp; Kir1.1 (GenBank accession no. NM_017023, 1211–1311), amplicon = 101 bp; Kir2.1 (GenBank accession no. NM_017296, 278–378), amplicon = 101 bp; Kir2.2 (GenBank accession no. NM_053981, 856–972), amplicon = 117 bp; Kir2.3 (GenBank accession no. NM_053870, 1129–1234), amplicon = 106 bp; Kir2.4 (GenBank accession no. NM_170718, 739–844), amplicon = 106 bp; Kir3.1 (GenBank accession no. NM_031610, 804–905), amplicon = 102 bp; Kir6.1 (GenBank accession no. NM_017099, 968–1074), amplicon = 107 bp; Kir6.2 (GenBank accession no. NM_031358, 1679–1781), amplicon = 103 bp; and GAPDH (GenBank accession no. NM_017008, 1533–1636), amplicon = 104 bp.

Measurements of changes in membrane potential: $DiBAC_3(4)$ studies. P1 myofibroblasts were incubated with normal Tyrode solution containing 1 μM $DiBAC_4(3)$ (30 min, 37°C). $DiBAC_4(3)$ is a bis-barbituric acid oxolol compound that partitions into the membrane as a function of membrane potential (12, 49). Hyperpolarization causes extrusion of the dye and decreased fluorescence, whereas depolarization causes enhanced fluorescence (1, 12, 49). Fluorescence was monitored with a fluorescent microscope (Olympus America) using the excitation and emission wavelengths of 470 and 525 nm, respectively. Relative fluorescence intensity was determined with OpenLab Software (Improvision). $DiBAC_4(3)$ was maintained at 1 μM in all solutions.

Collagen I gel deformation assays. Collagen I gels were prepared according to Takayama and Mizumachi (45). P1 myofibroblasts were maintained on gels for 7 days before being serum starved for 12 h. Gel deformation was then initiated at *time 0* by freeing gel edges with a scalpel. Individual gels were photographed with a Digital Camera (Nikon) at 0, 2, 4, 6, and 8 h. The surface area of each gel at each time was measured with custom software.

Assessment of myofibroblast number. P1 cells were allowed to grow to ~80% confluence in a Falcon tray and were then serum starved overnight. Cell number was determined after 24-h incubation in the presence of 1.7, 5.4, 10, or 20 mM $[K^+]_o$-Tyrode solution. Cells were trypsinized and counted with a Coulter cell counter (model ZM, Beckman Coulter) or a hemocytometer (Reichert).

Statistical analysis. Data are presented as means ± SE. Levels of statistical significance were assessed by unpaired Student's *t*-test. *P* values of 0.05 or less were considered statistically significant.

RESULTS

Currents recorded from adult rat ventricular fibroblasts and myofibroblasts. Using standard whole cell patch-clamp methods, we investigated the ionic basis for RMP in freshly dissociated adult rat ventricular fibroblasts as well as myofibroblasts that were maintained under culture conditions for 20 ± 1 days. Freshly dissociated ventricular fibroblasts are spherical and have an average capacitance of 6.3 ± 1.7 pF (n = 18). Their input resistance measured between −60 and −50 mV was 10.7 ± 2.3 GΩ (n = 23). With voltage-clamp steps (500 ms) applied in 10-mV increments between −140 and 30 mV, from a holding potential of −50 mV, measurements of peak currents yielded a sigmoidal *I-V* relationship (Fig. 1*A*). This suggested that at least two distinct types of currents were expressed in these cells. A representative family of currents from an individual fibroblast is shown in Fig. 1*A*, *inset*. At membrane potentials negative to approximately −60 mV, an inwardly rectifying current was recorded, whereas at membrane potentials positive to approximately −40 mV, a time- and voltage-dependent outward K^+ current was activated. This general pattern of K^+ currents was recorded in ~90% (33/35) of these fibroblasts. Approximately 70% (25/35) of these fibroblasts expressed a measurable inwardly rectifying current. No regenerative responses were recorded from any freshly dissociated ventricular fibroblasts. The time- and voltage-dependent outward K^+ currents have been studied in detail in a separate project in our laboratory (42). For this reason, their properties will not be further considered here.

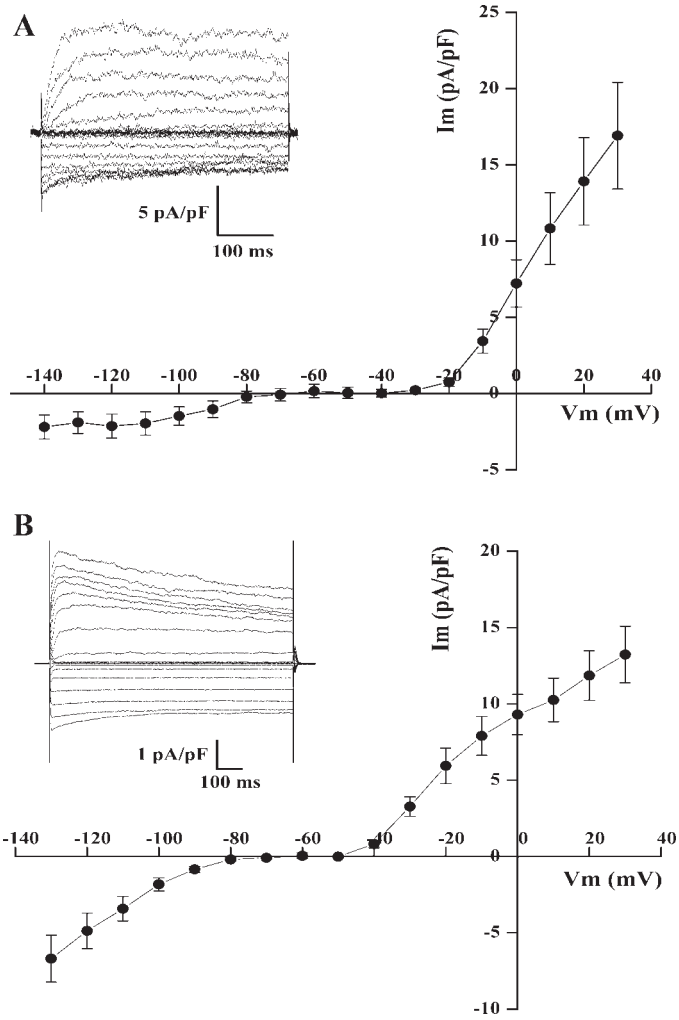

Fig. 1. Family of currents recorded using fibroblasts and myofibroblasts from ventricles of adult rats. *A*: currents (means ± SE) recorded with whole cell patch-clamp techniques from freshly dissociated ventricular fibroblasts. *B*: currents (means ± SE) recorded from ventricular myofibroblasts. *Insets*, representative families of currents from a single fibroblast (*A*) and a single myofibroblast (*B*). In each of these experiments, the cell was voltage clamped at −50 mV, and the membrane voltage (V_m) was then stepped in 10-mV increments in the range of −140 mV (*A*) or −130 mV (*B*) to 30 mV. All experiments were done at room temperature (22 ± 1°C). I_m, membrane current.

A similar pattern of currents was recorded from single adult rat ventricular myofibroblasts. When maintained under culture conditions for 20 ± 1 days, myofibroblasts spread and proliferate significantly and also develop numerous cellular processes. Individual myofibroblasts have a much larger capacitance (53.2 ± 9.4 pF, n = 20) than freshly dissociated fibroblasts. When individual myofibroblasts were voltage clamped at −50 mV and stepped (1 s) from −130 to 30 mV, both inwardly rectifying currents and outward time- and voltage-dependent K^+ currents were recorded in 95% (19/20) of these cells. Figure 1*B*, *inset*, shows a representative family of currents from a single myofibroblast. When considered as an entire population, myofibroblasts appeared to have larger inwardly rectifying current density than freshly dissociated fibroblasts [myofibroblasts: −6.7 ± 2.5 pA/pF (n = 20) vs. fibroblasts: −1.9 ± 0.7 pA/pF (n = 20) at −130 mV]. However, when only those fibroblasts with a measurable Kir current were considered, this difference was no longer apparent [myofibroblasts: −6.7 ± 2.5 pA/pF (n = 20) vs. fibroblasts: −6.3 ± 2.8 pA/pF (n = 7), at a membrane potential of −130 mV]. Cultured myofibroblasts did not exhibit regenerative electrophysiological responses when electrical stimuli were applied.

Kir current is modulated by variations in $[K^+]_o$ and blocked by Ba^{2+}. To more fully characterize the inwardly rectifying current(s) expressed in fibroblasts and myofibroblasts, responses to changes in $[K^+]_o$ were recorded and blockade by $BaCl_2$ was assessed. As shown in Fig. 2*A*, when a single fibroblast that expressed a strongly rectifying inward current was superfused with solutions containing increased $[K^+]_o$, the apparent reversal potential of this inwardly rectifying current shifted to more depolarized potentials. This cell was held at −50 mV, and currents were activated with 1-s voltage ramps from −140 to 50 mV. In 10 mM $[K^+]_o$, inward current was recorded at membrane potentials negative to −60 mV, and, in 25 and 75 mM $[K^+]_o$ solutions, larger inward currents were observed in the hyperpolarized range of membrane potentials.

An estimate of the reversal potentials (E_K) of these currents can be determined from the *I-V* relationships. In 25 and 75 mM $[K^+]_o$, the E_K was approximately −47 and approximately −23 mV, respectively. The corresponding E_K values are −67 mV (10 mM $[K^+]_o$), −44 mV (25 mM $[K^+]_o$); and −16 mV (75 mM $[K^+]_o$). On this basis, the predicted shift in E_K of a K^+-selective current would be 23 mV (10 vs. 25 mM $[K^+]_o$) and 51 mV (10 vs. 75 mM $[K^+]_o$). The recorded shifts in E_K were 17 mV (10 vs. 25 mM $[K^+]_o$) and 41 mV (10 vs. 75 mM $[K^+]_o$). A pattern of similar results was obtained from a single myofibroblast in which inwardly rectifying currents were stud-

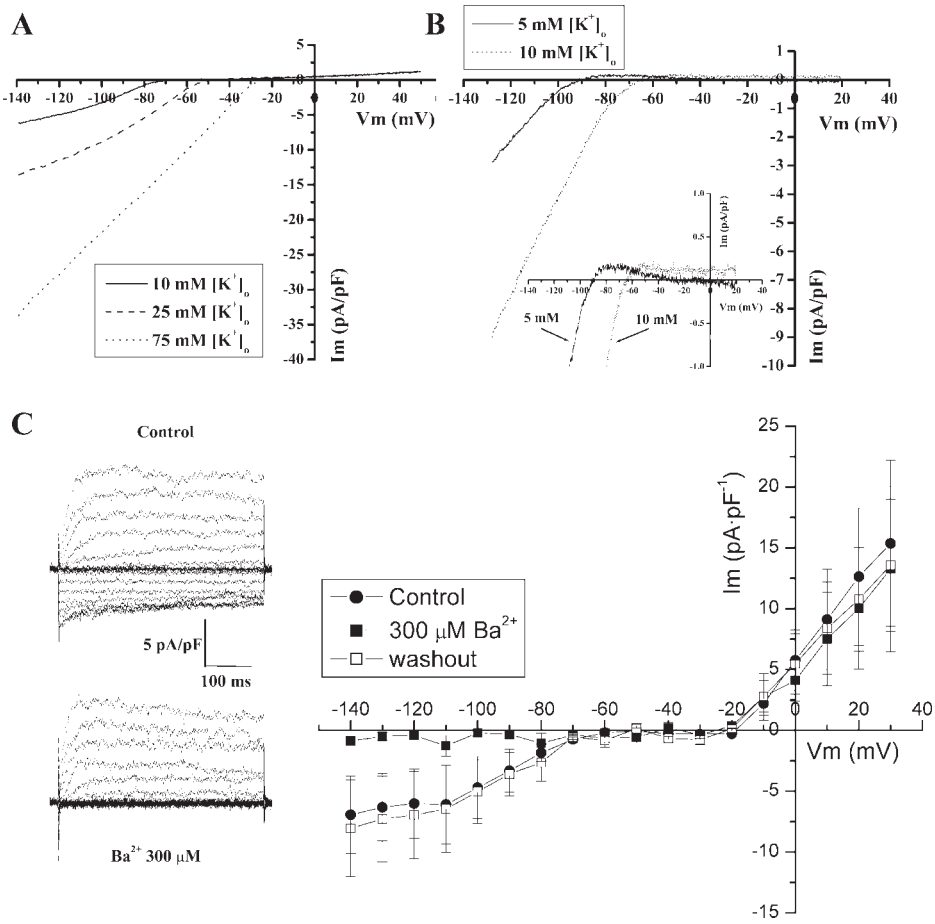

Fig. 2. Inwardly rectifying K^+ (Kir) currents are modulated by variations in external K^+ concentration ($[K^+]_o$) and are blocked by $BaCl_2$. Currents were activated by clamping the fibroblast at −50 mV and then applying a voltage ramp lasting 1 s from −140 to 50 mV. Note that varying $[K^+]_o$ from 10 to 25 or 75 mM caused a shift in the reversal potential of the inwardly rectifying current recorded in freshly dissociated ventricular fibroblasts (*A*) together with nonlinear changes in current size. *B*: difference currents resulting from $BaCl_2$ (10^{-4} M) application. These were recorded from a single myofibroblast in 5 and then 10 mM $[K^+]_o$. In these experiments, currents were activated by clamping the myofibroblast at −50 mV and then applying a voltage ramp lasting 1 s from −130 to 20 mV. The outward component of each Ba^{2+}-sensitive difference current is shown at high gain in the *inset* to illustrate the strong inward rectification. *C*: sensitivity of this K^+ current to Ba^{2+} block in fibroblasts is illustrated by the representative family of currents under control conditions (*top left*) and in the presence of 300 μM Ba^{2+} (*bottom left*, means ± SE, n = 6). In these experiments, each fibroblast was voltage clamped at −50 mV, and a series of 10-mV voltage-clamp steps was applied from −140 to 30 mV.

ied (Fig. 2*B*). In Fig. 2*B*, difference currents resulting from $BaCl_2$ (100 μM) application currents are plotted during superfusion with 5 and then 10 mM $[K^+]_o$. Again, the E_K is shifted to more depolarized potentials as $[K^+]_o$ was elevated: at 5 mM $[K^+]_o$, E_K was approximately −87 mV, whereas at 10 mM $[K^+]_o$, it is shifted to approximately −65 mV. The theoretical E_K values are −83 and −67 mV, respectively. The predicted shift in E_K for a K^+ current would be 16 mV (5 vs. 10 mM $[K^+]_o$), whereas the recorded shift was ~22 mV in this myofibroblast (Fig. 2*B*). These findings confirm that this inward current is carried by K^+.

Note that a small outward $BaCl_2$-sensitive difference current was recorded from myofibroblasts in both 5 and 10 mM $[K^+]_o$. This important result is illustrated in Fig. 2*B*, *inset*. It is this outward current that is responsible for modulating the resting potential. Although the peak magnitude of this current is small, it can maintain and regulate RMP as a result of the very high input resistance in single isolated fibroblasts and myofibroblasts.

In the experiment shown in Fig. 2*C*, the ability of low concentrations of Ba^{2+} to block the Kir current of fibroblasts was assessed. Figure 2*C*, *inset*, shows representative families of currents from a single fibroblast under control conditions (*top left*) and after exposure to 300 μM Ba^{2+} (*bottom left*). Application of 300 μM Ba^{2+} in the presence of 10 mM $[K^+]_o$ completely blocked the inward component of this family of currents. Fully reversible blocks of Kir current by 300 μM Ba^{2+} were consistently observed (closed squares, Fig. 2*C*) and was reversible (open squares, Fig. 2*C*). These data demonstrate that the K^+ currents recorded at hyperpolarized membrane potentials in rat ventricular fibroblasts and myofibroblasts are mainly due to expression of Kir channels.

mRNAs for Kir2.1 and Kv1.6 are expressed in ventricular myofibroblasts. To attempt to identify which K^+ channel subtypes/families generate these inwardly rectifying and time- and voltage-dependent outward K^+ currents, total RNA was isolated from first passage myofibroblasts. These RNA samples were then probed for the α-subunits of a number of Kir and voltage-gated K^+ (Kv) channels using primers developed against rat genes. As shown in Fig. 3*A*, qualitative RT-PCR experiments revealed that, of the Kv1 channel subtypes tested, Kv1.6 transcripts were abundantly expressed in rat ventricular myofibroblasts, and Kv1.1, Kv1.2, and Kv1.5 transcripts were expressed at lower levels. Quantitative real-time PCR analysis also showed abundant expression of Kv1.6, with expression of Kv1.6 relative to GAPDH of 0.032 ± 0.002 (n = 3) (Fig. 3*B*). The expression levels of the other Kv1 subtypes were <0.003 (n = 3) (Fig. 3*B*). Similarly, in rat ventricular myofibroblasts, qualitative RT-PCR experiments revealed that Kir2.1 and Kir6.1 transcripts were expressed, whereas other transcripts examined (Kir1.1, Kir2.2, Kir2.3, Kir2.4, Kir3.1, and Kir6.2) were not (Fig. 3*C*). Quantitative real-time PCR analysis also revealed significant expression of Kir2.1 and Kir6.1. The expression of Kir2.1 and Kir6.1 was 0.008 ± 0.002 and 0.006 ± 0.001, respectively (n = 3), and the expression level of the other Kir channel subtypes was <0.003 (n = 3) (Fig.

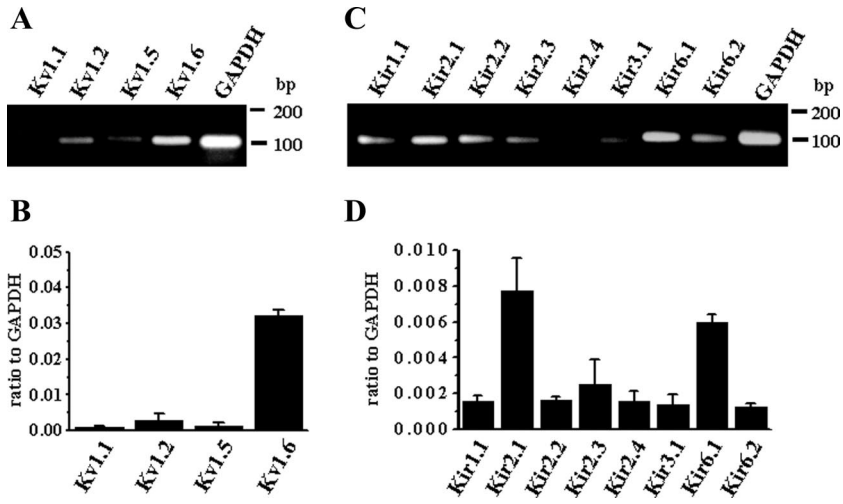

Fig. 3. Molecular identification of K^+ Channel α-subunits in rat ventricular myofibroblasts. RT-PCR was used to detect delayed rectifier-type voltage-gated K^+ (Kv)1 channel transcripts (*A* and *B*) and Kir channel transcripts (*C* and *D*) using RNA from adult rat ventricular myofibroblasts. PCR products were generated through the use of rat gene-specific primers for Kv1.1, Kv1.2, Kv1.5, Kv1.6, Kir1.1, Kir2.1, Kir2.2, Kir2.3, Kir2.4, Kir3.1, Kir6.1, and Kir6.2. A 100-bp molecular weight marker was used to estimate the size of the amplicon, as shown on the *right* of *A* and *C*. PCR products were sequenced to confirm their identity. RT-PCR performed in the presence of GAPDH-specific primers demonstrates that the products are representative of RNA. *C* and *D*: quantitative RT-PCR for Kv1 and Kir channel α-subunits relative to GAPDH from the same RNA preparation of rat cardiac myofibroblasts. Results are expressed as means ± SE.

3*D*). These findings, in conjunction with our electrophysiological results, strongly suggest that Kv1.6 and Kir2.1 are responsible for delayed rectifier and Kir currents in rat ventricular myofibroblasts, respectively.

Kir current is the primary determinant of RMP in fibroblasts and myofibroblasts. Kir current is the primary determinant of RMP in many cell types (cf. Refs. 1, 8, and 38). In 5.4 mM $[K^+]_o$, the RMP of myofibroblasts was -80 ± 1.8 ($n = 20$), a value similar to the theoretical E_K [approximately −83 mV: 22°C, assuming an internal K^+ concentration ($[K^+]_i$) of ~139 mM]. The time- and voltage-dependent outward K^+ current was recorded only at membrane potentials positive to −40 mV. The average RMP of freshly dissociated ventricular fibroblasts in 10 mM $[K^+]_o$ was -65 ± 5 mV ($n = 14$), which is close the theoretical E_K (approximately −67 mV: 22 °C, assuming $[K^+]_i$ ~139 mM). Most of our experiments were carried out in the presence of 10 mM $[K^+]_o$ to increase the amplitude of K^+ currents and thus enhance identification of their biophysical properties.

Decreasing $[K^+]_o$ hyperpolarizes and increasing $[K^+]_o$ depolarizes myofibroblasts. The role of membrane potential in modulating physiological functions of fibroblast and myofibroblast is not known. We began to investigate this important question by changing $[K^+]_o$ and measuring myofibroblast functions in terms of proliferation and contractility. As shown in Fig. 4, membrane potential in myofibroblasts was modulated by varying $[K^+]_o$. When $[K^+]_o$ was elevated in the superfusate of first passage myofibroblasts, the $DiBAC_3(4)$ fluorescence increased, indicating a depolarization (Fig. 4*A*; from 5.4 to 20 mM; and Fig. 4*B*: from 5 to 15 mM $[K^+]_o$). Conversely, fluorescent intensity decreased, indicating a hyperpolarization, when $[K^+]_o$ was decreased (to 1.7 mM, Fig. 4*A*; or 1.5 mM, Fig. 4, *B* and *C*). These changes in dye intensity were reversible when $[K^+]_o$ was returned to control levels (Fig. 4, *B* and *C*). On average, $DiBAC_3(4)$ intensity increased by 11 ± 2% ($n = 26$) when $[K^+]_o$ was increased from 5.4 to 20 mM. Lowering $[K^+]_o$ to 1.7 mM resulted in an 11 ± 1% ($n = 25$) decrease in $DiBAC_3(4)$ signal intensity. These data indicate that modulation of $[K^+]_o$ modulates membrane potential; increased $[K^+]_o$ can cause depolarization, whereas decreased $[K^+]_o$ results in hyperpolarization in ventricular myofibroblasts.

Decreasing $[K^+]_o$ enhances myofibroblast proliferation and/or survival. The functional consequences of modulating membrane potential by altering $[K^+]_o$ have been evaluated. Cardiac myofibroblasts can proliferate in culture (48–49). Accordingly, the effect of altering $[K^+]_o$ and membrane potential on myofibroblast number was studied. When first passage myofibroblasts were incubated for 24 h with either 1.7, 10, or 20 mM $[K^+]_o$ solutions, the total number of myofibroblasts was significantly different from control (5.4 mM) $[K^+]_o$ conditions. As shown in Fig. 5, when $[K^+]_o$ was decreased to 1.7 mM (open bar), the number of myofibroblasts was significantly increased relative to control numbers [solid bar; 85,102 ± 4,038 cells/well ($n = 6$) control conditions compared with 137,093 ± 4,962 cells/well ($n = 6$) with 1.7 mM $[K^+]_o$ present, $P < 0.01$]. In contrast, when $[K^+]_o$ was increased to either 10 (hatched bar) or 20 (crosshatched bar) mM, the number of myofibroblasts decreased relative to control (10 mM $[K^+]_o$, 52,408 ± 4,764 cells/well, $n = 6$, $P < 0.01$ relative to control; 20 mM $[K^+]_o$, 51,763 ± 3,481 cells/well, $n = 6$, $P < 0.01$ relative to control). These findings indicate that exposure to low $[K^+]_o$, which induces hyperpolarization, can enhance myofibroblast proliferation and/or survival. In contrast, exposure to elevated $[K^+]_o$, which produces a depolarization, did not promote proliferation and/or may have compromised survival. In this assay, cell number were determined 24 h after each maneuver, with no distinction being made between proliferation versus survival.

Increasing $[K^+]_o$ enhances myofibroblast contractility. Depolarization would be expected to result in myofibroblast contraction, as judged by a collagen I gel deformation assay (8). Decreased collagen I gel surface area has been shown to be an indirect but reliable indication of myofibroblast contraction (32–33, 45–46). As shown in Fig. 6, when myofibroblasts were placed on collagen I gels, the gel surface area decreased significantly over 8 h under control $[K^+]_o$ conditions (open circles, 140.4 ± 2.5 mm^2 at *time 0*, $n = 24$, vs. 93.0 ± 2.6 mm^2 at 8 h, $n = 8$, $P < 0.001$). These results confirm that these myofibroblasts exhibited normal contractile activity. When exposed to 20 mM $[K^+]_o$ (closed circles) for 8 h, the average surface area of the collagen I gels was significantly smaller than under control conditions (86.7 ± 2.1 mm^2 at 20 mM $[K^+]_o$ vs. 93.0 ± 2.6 mm^2 at 5.4 mM $[K^+]_o$, $n = 8$, $P = 0.03$),

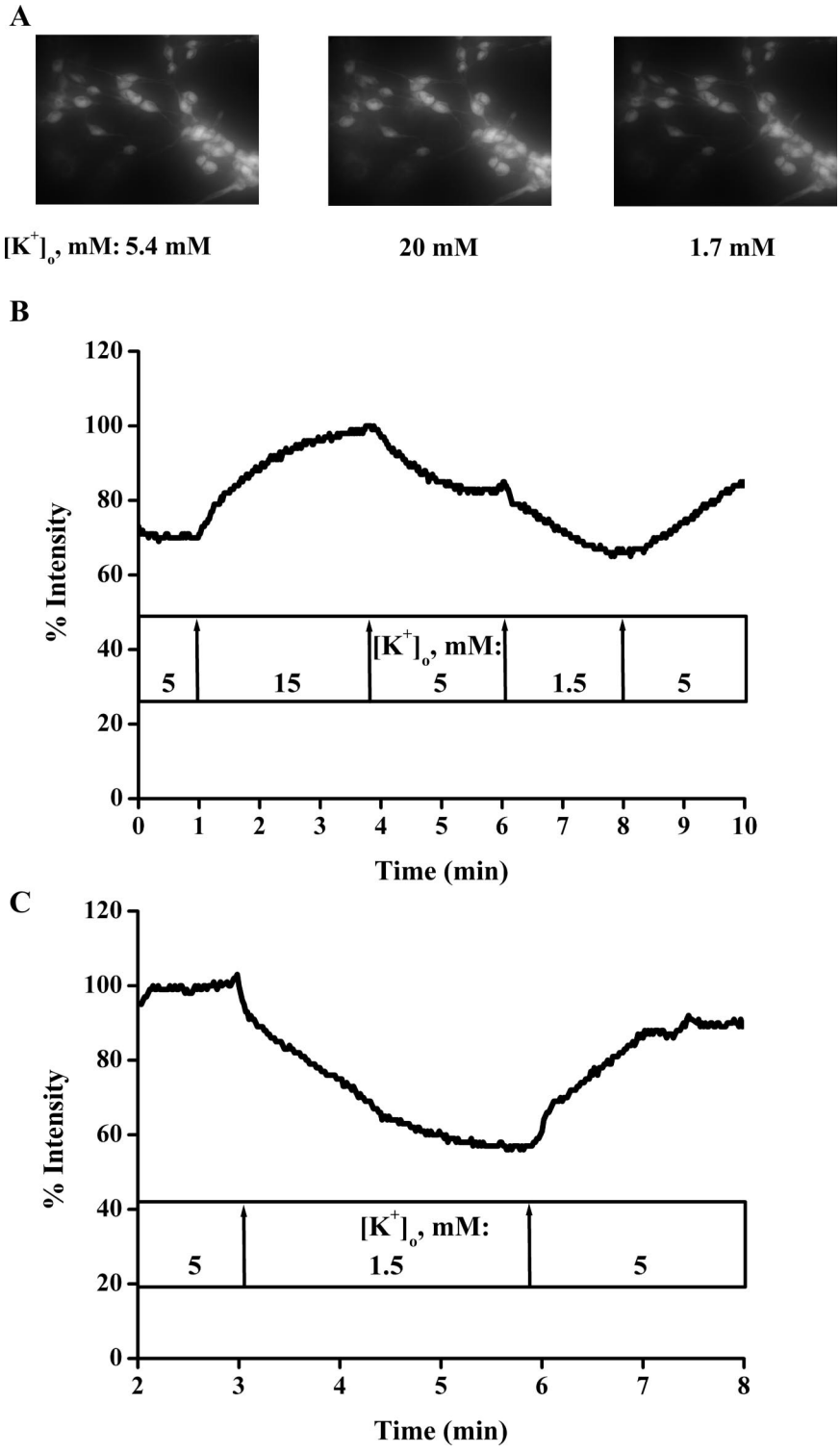

Fig. 4. Effect of varying $[K^+]_o$ on membrane potential in ventricular myofibroblasts. *A*: representative photomicrographs of ventricular myofibroblasts exposed to 1 μM $DiBAC_4(3)$ in 5.4 (*left*), 20 (*middle*), and 1.7 (*right*) mM $[K^+]_o$. $DiBAC_4(3)$ emission increased when $[K^+]_o$ was raised (*A* and *B*, *middle*; *C*, *left* portion) and decreased when $[K^+]_o$ was decreased (*A* and *B*, *right* portion; *C*, *middle*).

suggesting that depolarization had significantly enhanced myofibroblast contractile activity. Exposure of myofibroblasts for 8 h to 10 ng/ml transforming growth factor (TGF)-β, a very potent contractile agonist (18, 45–46), produced a reduction in collagen I gel surface area approximately equivalent to that observed in 20 mM $[K^+]_o$ conditions (TGF-β: 90.4 ± 1.4 mm^2, $n = 8$, vs. 20 mM $[K^+]_o$: 86.7 ± 2.1 mm^2, $n = 8$, not significant). In combination, these data indicate that depolarization enhances contractility of myofibroblasts.

DISCUSSION

Summary of main findings. Our results demonstrate that the major ionic currents in freshly isolated adult rat ventricular

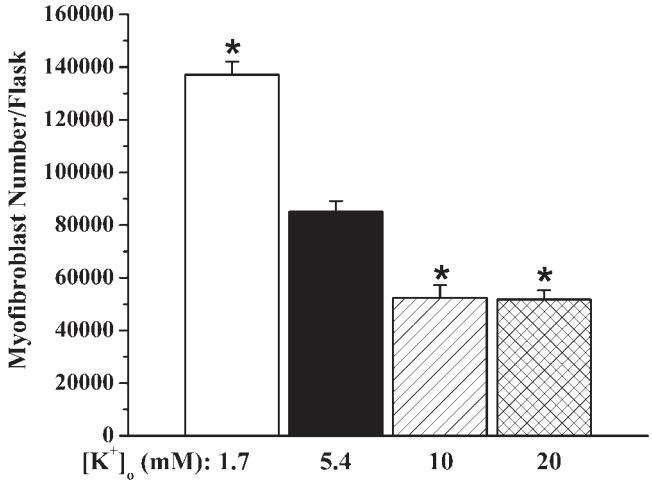

Fig. 5. Effect of varying $[K^+]_o$ on ventricular myofibroblast proliferation measured as the total number of myofibroblasts. Reduction of $[K^+]_o$ from 5.4 (solid bar) to 1.7 mM (open bar) resulted a significant increase in the number of myofibroblasts per well measured after 24-h incubation. Elevating $[K^+]_o$ from 5.4 (solid bar) to 10 (hatched bar) or 20 mM (crosshatched bar) resulted in a significant decrease in the number of myofibroblasts per well. $*P < 0.01$ relative to 5.4 mM $[K^+]_o$.

fibroblasts and myofibroblasts under these cell culture conditions include a Kir current (which is blocked by Ba^{2+} at low concentrations) and a time- and voltage-gated outward K^+ current (which is activated when these cells are depolarized). Consistent with these electrophysiological findings, mRNA for both Kir2.1 and Kv1.6 channels is expressed in these ventricular myofibroblasts. Variation of $[K^+]_o$ changes membrane potential and modulates some physiological functions in these myofibroblasts. Low $[K^+]_o$ (1.5 or 1.7 mM) causes hyperpolarization of myofibroblasts. Under these conditions, significantly greater numbers of myofibroblasts were present after 24-h incubation. In contrast, 15 or 20 mM $[K^+]_o$-Tyrode solution, which caused a depolarization, resulted in significantly fewer myofibroblasts after 24-h incubation. Similar elevated $[K^+]_o$ conditions applied in a gel contraction assay resulted in enhanced collagen I gel deformation, indicating that depolarization can enhance myofibroblast contractility.

Expression of K^+ currents in fibroblasts and myofibroblasts. This is the first report of a Kir current in cardiac fibroblasts or myofibroblasts. Only a few previous studies have investigated K^+ current expression in cardiac fibroblasts. In cultured neonatal rat cardiac fibroblasts (37) and in freshly dissociated adult rat atrial fibroblasts (22), no inward currents were recorded at hyperpolarized potentials. However, in (noncardiac) fibroblasts and myofibroblasts, this type of Kir current has been described. Fibroblasts and myofibroblasts are present in all organs (for detailed reviews, see Refs. 36, 39, 41, and 46) and include macroglial cells of the brain (30, 36), hepatic stellate cells, and vascular pericytes, among many others. In addition, a number of cell lines have been derived from fibroblasts, including normal rat kidney (NRK) myofibroblasts (19). Kir currents have been described in astrocytes (26), oligodendrocytes (30), hepatic stellate cells (24), coronary microvessel pericytes maintained under culture conditions (4), and NRK myofibroblasts (18).

In ventricular fibroblasts and myofibroblasts, we consistently recorded time- and voltage-dependent outward K^+ currents. These K^+ currents are the focus of detailed biophysical and pharmacological studies in our laboratory (42). These results show that this K^+ current has slow time- and voltage-dependent activation kinetics. It exhibits C-type inactivation as judged by its modulation after changes in $[K^+]_o$ as well as by block by extracellular tetraethylammonium (42). Previous studies done using cultured neonatal rat cardiac fibroblasts identified a somewhat similar outwardly rectifying current (37). Analogous Kv currents have also been described in numerous noncardiac types of fibroblasts and myofibroblasts, including astrocytes (26), oligodendrocytes (30), hepatic stellate cells (24), NRK myofibroblasts (18), and coronary microvessel pericytes (4). In contrast, no Kv currents have been recorded from freshly dissociated rat atrial fibroblasts (23).

Inwardly rectifying K^+ current is a primary determinant of RMP. Kir2.1, the classic strongly Kir channel, has been identified in numerous cell types. It was first described in skeletal muscle (25), and the molecular transcript responsible for it was cloned from J744 cells, a mouse macrophage cells line (31). Kir channels may serve a variety of functions, including maintaining RMP, modulating the threshold for cellular excitability, and contributing to tissue K^+ homeostasis (for a review, see Ref. 38). In both adult rat ventricular fibroblasts and myofibroblasts, Kir current is the primary determinant of RMP. Previous papers reported that in neonatal rat cardiac fibroblasts, RMP was -20 to -30 mV (37), whereas in atrial fibroblasts, RMP was -37 ± 3 mV (21). No measurable Kir currents were expressed in these cardiac fibroblasts. In noncardiac fibroblasts and myofibroblasts in which Kir current has been recorded, RMPs were more similar to the values we report for ventricular fibroblasts and myofibroblasts. For example, in hepatic stellate cells perfused with 5.4 mM $[K^+]_o$-Tyrode solution, RMP was -81 ± 5 mV (24). These authors concluded that Kir current was the primary determinant of RMP in these cells. Similarly, in NRK myofibroblasts, Kir current modulates RMP, which is approximately -70 mV (18). In contrast, average RMP in pericytes from the coronary circulation is -49 ± 10 mV in 5.4 mM $[K^+]_o$-Tyrode solution (4), suggesting that in these cells, Kir current contributes to, but is not the primary determinant of, RMP.

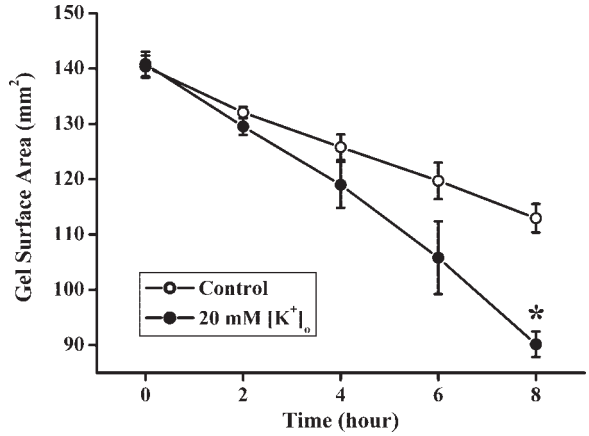

Fig. 6. Effect of raising $[K^+]_o$ on ventricular myofibroblast contractility determined using an assay based on collagen I gel deformation. Changes in collagen I gel surface area over 8 h are plotted in high $[K^+]_o$ (20 mM) vs. control $[K^+]_o$ (5.4 mM). $*P < 0.01$ relative to control collagen I gel surface area measured 8 h after selected changes were made in $[K^+]_o$.

In our study, Kir currents were recorded from 71% of the freshly dissociated ventricular fibroblasts studied. In those ventricular fibroblasts in which no Kir current was recorded, RMP was more depolarized than in cells that did express Kir current (-34 ± 2 mV, $n = 7$, vs. -65 ± 5 mV, $n = 14$, respectively). In fibroblasts in which no Kir current was recorded, a different ionic mechanism must account for the RMP. The time- and voltage-dependent outward K^+ current, which is activated at membrane potentials positive to -40 mV, is a possible candidate. Another plausible contributor to RMP is the electrogenic current of the Na^+/K^+ pump (10). The basis for the RMP together with the reasons underlying the heterogeneity in Kir current expression is the focus of further experiments in our laboratory. In these investigations, attempts to account and control for the prominent effects on fibroblast phenotype of cell culture conditions and imposed mechanical activity are being included (18).

Changing membrane potential modulates physiological functions in myofibroblasts. The results of our study provide the first demonstration that changing membrane potential can modulate physiological functions in cardiac myofibroblasts. In noncardiac fibroblasts and myofibroblasts (and many other cells), modulation of physiological function after manipulation of membrane potential is normal and expected. For example, K^+ current appears to be essential in maintaining astrocytes (34), oligodendrocytes (30), and a fibroblast cell line (35) in defined proliferative states. In each of these cell types, blocking K^+ current resulted in inhibition of proliferation. Similarly, in activated microglia in tissue culture, inhibition of Kir current resulted in inhibition of proliferation (40). We observed that when $[K^+]_o$ was increased, the depolarization resulted in enhanced ventricular myofibroblast contractility, as judged by enhanced collagen I gel deformation (Fig. 6). A somewhat similar relationship between depolarization and contractility has been described in activated hepatic stellate cells. Depolarization can enhance contractile activity of both native activated hepatic stellate cells and those in culture conditions (2, 3).

Fibroblast and myofibroblast physiology in vivo. Detailed information concerning the ionic basis for membrane potential, and the effect of modulating membrane potential on physiological function in ventricular fibroblasts and myofibroblasts is essential for an understanding of how these cells function in vivo. Recent evidence has indicated that ventricular fibroblasts communicate to other fibroblasts as well as to cardiomyocytes via gap junctions (6, 17). Electrophysiological coupling mediated by gap junctions has also been described among myofibroblasts within infarction scars of sheep hearts (7). Under culture conditions, neonatal rat cardiac fibroblasts can electrically couple with cardiomyocytes, resulting in electrotonic changes of fibroblast membrane potential and propagation of action potentials across fibroblasts separating cardiac myocytes (16, 37). It is of interest to determine whether, and under what conditions, modulation of fibroblast and/or myofibroblast membrane potential due to this electrotonic coupling with cardiomyocytes does occur within the mammalian ventricle. These electrotonic changes (depolarizations) could influence physiological function of both fibroblasts and myofibroblasts. It is now well known that mechanical forces experienced by fibroblasts can alter their function, perhaps by modulating membrane potential or regulating intrinsic responses to autocrine or paracrine factors in the tissue environment. It is also likely that variations in the chemical and/or electrophysiological milieu surrounding the fibroblast or myofibroblast in vivo affect their membrane potential and physiological function (18). For example, elevation in $[K^+]_o$ within the ventricle is observed in the first few minutes of ischemia (12). On the basis of our results, an increase in $[K^+]_o$ would affect membrane potential and functional responses of intraventricular fibroblasts.

In summary, we demonstrated that K^+ currents expressed in adult rat ventricular fibroblasts and myofibroblasts have important physiological roles. In most of these cells, Kir current is the primary determinant of RMP, and changes in $[K^+]_o$ can significantly alter membrane potential. In turn, change of membrane potential modulates both proliferation and contractility in myofibroblasts. Ongoing studies are investigating the effects of electrical coupling of myocytes with fibroblasts and/or myofibroblasts. In the future, it will be essential to integrate these findings with the interesting, important capabilities of tissue engineering paradigms so that fibroblast function can be assessed in a more physiological two- or three-dimensional growth pattern (18). Previous studies have shown that fibroblast and myofibroblast function and phenotype is strongly regulated by both their microenvironment and the surrounding matrix.

ACKNOWLEDGMENTS

The authors are grateful to Dr. Anders Nygren for providing the computer program that was used to measure the collagen I gel surface area.

GRANTS

This study was supported by grants from the Canadian Institutes of Health Research (to I. M. C. Dixon and W. R. Giles), the Heart and Stroke Foundation of Canada (to I. M. C. Dixon, W. R. Giles, and L. Chilton), the Alberta Heritage Foundation for Medical Research (to W. R. Giles and L. Chilton), and Japanese Ministry of Health and Welfare Research Grant for Cardiovascular Diseases 12C-1 (to Y. Imaizumi) as well as the Research Chair sponsored by the Heart and Stroke Foundation of Alberta and the Northwest Territories (to W. R. Giles). D. Freed is a recipient of a Postdoctoral Fellowship for the Manitoba Health Research Council, and I. M. C. Dixon is a Scholar of the Myles Robinson Memorial Heart Fund.

REFERENCES

1. **Baczko I, Giles WR, and Light PE.** Resting membrane potential regulates Na^+-Ca^{2+} exchange-mediated Ca^{2+} overload during hypoxia-reoxygenation in rat ventricular myocytes. *J Physiol* 550: 889–898, 2003.
2. **Bataller R, Nicolás JM, Ginès P, Görbig MN, Garcia-Ramallo E, Lario S, Tobias E, Pinzani M, Thomas AP, Arroyo V, and Rodés J.** Contraction of human hepatic stellate cells activated in culture: a role for voltage-operated calcium channels. *J Hepatol* 29: 398–408, 1998.
3. **Bataller R, Gasull X, Ginès P, Hellemans K, Görbig MN, Nicolás JM, Sancho-Bru P, De Las Heras D, Gual A, Geerts A, Arroyo V, and Rodés J.** In vitro and in vivo activation of rat hepatic stellate cells results in de novo expression of L-type voltage-operated calcium channels. *Hepatology* 33: 956–962, 2001.
4. **Beckerath N, Nees S, Neumann FJ, Krebs B, Juchemm G, and Schömig A.** An inward rectifier and a voltage-dependent K^+ current in single, cultured pericytes from bovine heart. *Cardiovasc Res* 46: 569–578, 2000.
5. **Brilla CG, Maisch B, Zhou G, and Weber KT.** Hormonal regulation of cardiac fibroblast function. *Eur Heart J* 16: 45–50, 1995.
6. **Camelliti P, Green CR, LeGrice I, and Kohl P.** Fibroblast network in rabbit sinoatrial node. *Circ Res* 94: 828–835, 2004.
7. **Camelliti P, Devlin GP, Matthews KG, Kohl P, and Green CR.** Spatially and temporally distinct expression of fibroblast connexins after sheep ventricular infarction. *Cardiovasc Res* 62: 415–425, 2004.
8. **Chilton L, Kargacin G, Dixon I, Clark R, and Giles WR.** An inwardly rectifying K^+ current modulates membrane potential in cultured rat cardiac fibroblasts (Abstract). *Biophys J* 84: 225A, 2003.

9. **Chilton L, George E, MacCannell D, Dixon IMC, Clark RB, and Giles WR.** Elevated $[K^+]_o$ enhances cultured adult rat cardiac myofibroblast contraction (Abstract). *J Physiol* 551P: PC35, 2003.
10. **Del Corsso C and Varanda WA.** The resting potential of mouse Leydig cells: role of an electrogenic Na^+/K^+ pump. *J Membr Biol* 191: 123–131, 2003.
11. **Ellmers LJ, Knowles JW, Kim HS, Smithies O, Maeda N, and Cameron VA.** Ventricular expression of natriuretic peptides in $Npr1^{-/-}$ mice with cardiac hypertrophy and fibrosis. *Am J Physiol Heart Circ Physiol* 283: H707–H714, 2002.
12. **Epps DE, Wolfe ML, and Groppi V.** Characterization of the steady-state and dynamic fluorescence properties of the potential-sensitive dye bis-1,3-dibutylbarbituric acid trimethine oxonol [$Dibac_4(3)$] in model systems and cells. *Chem Phys Lipids* 69: 137–150, 1994.
13. **Fozzard HA and Makielski JC.** The electrophysiology of acute myocardial ischemia. *Annu Rev Med* 36: 275–284, 1985.
14. **Frangogiannis NG, Smith CW, and Entman ML.** The inflammatory response in myocardial infarction. *Cardiovasc Res* 53: 31–47, 2002.
15. **Freed DH.** *Cardiotropin-1: Expression in Post-MI Heart and Effect on Primary Adult Cardiac Myofibroblasts In Vitro.* (PhD thesis). Winnipeg, Manitoba, Canada: University of Manitoba, 2003.
16. **Gaudesius G, Miragoli M, Thomas SP, and Rohr S.** Coupling of cardiac electrical activity over extended distances by fibroblasts of cardiac origin. *Circ Res* 93: 421–428, 2003.
17. **Goldsmith EC, Hoffman A, Morales MO, Potts JD, Price RL, McFadden A, Rice M, and Borg TK.** Organization of fibroblasts in the heart. *Dev Dyn* 230: 787–794, 2004.
18. **Grinnell F.** Fibroblast biology in three-dimensional collagen matrices. *Trends Cell Biol* 13: 264–269, 2003.
19. **Harks EGA, Torres JJ, Cornelisse LN, Ypey DL, and Theuvenet APR.** Ionic basis for excitability in normal rat kidney (NRK) fibroblasts. *J Cell Physiol* 196: 493–503, 2003.
20. **Kamkin A, Kiseleva I, Wagner KD, Scholz H, Theres H, Kazanski V, Lozinsky I, Günther J, and Isenberg G.** Mechanically induced potentials in rat atrial fibroblasts depend on actin and tubulin polymerization. *Pflügers Arch* 442: 487–497, 2001.
21. **Kamkin A, Kiseleva I, Wagner KD, Pylaev A, Leiterer KP, Theres H, Scholz H, Güther J, and Isenberg G.** A possible role for atrial fibroblasts in postinfarction bradycardia. *Am J Physiol Heart Circ Physiol* 282: H842–H849, 2002.
22. **Kamkin A, Kiseleva I, and Isenberg G.** Activation and inactivation of a non-selective cation conductance by local mechanical deformation of acutely isolated cardiac fibroblasts. *Cardiovasc Res* 57: 793–803, 2003.
23. **Kamkin A, Kiseleva I, Wagner KD, Lozinsky I, Güther J, and Scholz H.** Mechanically induced potentials in atrial fibroblasts from rat hearts are sensitive to hypoxia/ reoxygenation. *Pflügers Arch* 446:169–174, 2003.
24. **Kashiwagi S, Suematsu M, Wakabayashi Y, Kawada N, Tachibana M, Koizumi A, Inoue M, Ishimura Y, and Kaneko A.** Electrophysiological characterization of cultured hepatic stellate cells in rats. *Am J Physiol Gastrointest Liver Physiol* 272: G742–G750, 1997.
25. **Katz B.** Les constants electriques de la membrane du muscle. *Arch Sci Physiol* 307: 190–203, 1949.
26. **Kimelberg HK, Schools GP, Cai Z, and Zhou M.** Freshly isolated astrocyte (FIA) preparations: a useful single cell system for studying astrocyte properties. *J Neurosci Res* 61: 577–587, 2000.
27. **Kiseleva I, Kamkin A, Kohl P, and Lab MJ.** Calcium and mechanically induced potentials in fibroblasts of rat atrium. *Cardiovasc Res* 32: 98–111, 1996.
28. **Kiseleva I, Kamkin A, Pylaev A, Kondratjev D, Leiterer KP, Theres H, Wagner KD, Persson PB, and Gunther J.** Electrophysiological properties of mechanosensitive atrial fibroblasts from chronic infarcted rat heart. *J Mol Cell Cardiol* 30: 1083–1093, 1998.
29. **Kohl P, Kamkin AG, Kiseleva IS, and Noble D.** Mechanosensitive fibroblasts in the sino-atrial node region of rat heart: interaction with cardiomyocytes and possible role. *Exp Physiol* 79: 943–956, 1994.
30. **Knutson P, Ghiani CA, Zhou JM, Gallo V, and McBain CJ.** K^+ channel expression and cell proliferation are regulated by intracellular sodium and membrane depolarization in oligodendrocyte progenitor cells. *J Neurosci* 17: 2669–2682, 1997.
31. **Kubo Y, Baldwin TJ, Jan YN, and Jan LY.** Primary structure and functional expression of a mouse inward rectifier potassium channel. *Nature* 362: 127–133, 1993.
32. **Lijnen P, Petrov V, and Fagard R.** In vitro assay of collagen gel contraction by cardiac fibroblasts in serum-free conditions. *Methods Find Exp Clin Pharmacol* 23: 377–382, 2001.
33. **Nunohiro T, Ashizawa N, Graf K, Hsueh WA, and Yano K.** Angiotensin II promotes integrin-mediated collagen gel contraction by adult rat cardiac fibroblasts. *Jpn Heart J* 40: 461–469, 1999.
34. **Pappas CA, Ulrich N, and Sontheimer H.** Reduction of glial proliferation by K^+ channel blockers is mediated by changes in pH_i. *Neuro Report* 6: 193–196, 1994.
35. **Peña TL, Chen SH, Konieczny SF, and Rane SG.** Ras/MEK/ERK upregulation of the fibroblast KCa channel FIK is a common mechanism for basic fibroblast growth factor and transforming growth factor β suppression of myogenesis. *J Biol Chem* 275: 13677–13682, 2000.
36. **Powell DW, Mifflin RC, Valentich JD, Crowe SE, Saada JL, and West AB.** Myofibroblasts. I. Paracrine cells important in health and disease. *Am J Physiol Cell Physiol* 277: C1–C19, 1999.
37. **Rook MB, van Ginneken ACG, de Jonge B, el Aoumari A, Gros D, and Jongsma HJ.** Differences in gap junction channels between cardiac myocytes, fibroblasts, and heterologous pairs. *Am J Physiol Cell Physiol* 263: C959–C977, 1992.
38. **Ruppersberg JP.** Intracellular regulation of inward rectifier K^+ channels. *Pflügers Arch* 441: 1–11, 2000.
39. **Sappino AP, Schürch W, and Gabbiani G.** Differentiation repertoire of fibroblastic cells: expression of cytoskeletal proteins as marker of phenotypic modulations. *Lab Invest* 63: 144–1161, 1990.
40. **Schlichter LC, Sakellaropoulos G, Ballyk B, Pennefather PS, and Phipps DJ.** Properties of K^+ and Cl^- channels and their involvement in proliferation of rat microglial cells. *Glia* 17: 225–236, 1996.
41. **Schmitt-Gräff A, Desmoulière A, and Gabbiani G.** Heterogeneity of myofibroblastic phenotypic features: an example of fibroblastic cell plasticity. *Virchows Arch* 425: 3–24, 1994.
42. **Shibukawa Y, Chilton L, MacCannell D, Clark RB, and Giles W.** Biophysical properties of K^+ currents in cardiac fibroblasts. *Biophys J*. In press.
43. **Sun Y and Weber KT.** RAS and connective tissue in the heart. *Int J Biochem Cell Biol* 35: 919–931, 2003.
44. **Sun Y, Kiani MF, Postlethwaite AE, and Weber KT.** Infarct scar as living tissue. *Basic Res Cardiol* 97: 343–347, 2002.
45. **Takayama Y and Mizumachi K.** Effects of lactoferrin on collagen gel contractile activity and myosin light chain phosphorylation in human fibroblasts. *FEBS Lett* 508: 111–116, 2001.
46. **Tomasek JJ, Gabbiani G, Hinz B, Chaponnier C, and Brown RA.** Myofibroblasts and mechanoregulation of connective tissue remodeling. *Nat Rev Drug Discov* 3: 349–363, 2002.
47. **Wang J, Seth A, and McCulloch CA.** Force regulates smooth muscle actin in cardiac fibroblasts. *Am J Physiol Heart Circ Physiol* 279: H2776–H2785, 2000.
48. **Wang J, Chen H, Seth A, and McCulloch CA.** Mechanical force regulation of myofibroblast differentiation in cardiac fibroblasts. *Am J Physiol Heart Circ Physiol* 285: H1871–H1881, 2003.
49. **Yamada A, Gaja N, Ohya S, Muraki K, Narita H, Ohwada T, and Imaizumi Y.** Usefulness and limitation of $DiBAC_4(3)$, a voltage-sensitive fluorescent dye, for the measurement of membrane potentials regulated by recombinant large conductance Ca^{2+}-activated K^+ channels in HEK293 cells. *Jpn J Pharmacol* 86: 342–350, 2001.
50. **Zak R.** Cell proliferation during cardiac growth. *Am J Cardiol* 31: 211–219, 1973.